The ideal sliding dynamics of a stand alone synchronous generator

A. Dòria-Cerezo*, E. Fossas** and R.S. Muñoz-Aguilar***
*Department of Electrical Engineering and the Institute of Industrial and Control Engineering, Universitat Politècnica de Catalunya, Spain
**Department of Automatic Control and the Institute of Industrial and Control Engineering, Universitat Politècnica de Catalunya, Barcelona, Spain
***Department of Electrical Engineering, Universitat Politècnica de Catalunya, Spain
{arnau.doria, enric.fossas, raul.munoz-aguilar}@upc.edu

Summary. The closed loop dynamics of a sliding-mode controlled stand alone synchronous generator with a resistive load is studied in this paper. The resulting dynamics is piecewise continuous, robust in front of parameter and load variations and performs a good regulation of the output variable. In the ideal case we can find limit cycles that may remain when actuators saturation effects are considered. Along the paper, numerical simulations and experimental results illustrate the complexity of the encountered behavior.

Introduction

This paper deals with the analysis of the closed loop dynamics of a sliding mode controlled stand-alone wound rotor synchronous generator (WRSG) feeding a resistive load [1]. As reported in [2], sliding mode control is an appropriate technique to control electrical machines because the actuators are power converters which supply the electrical machine with discontinuous voltages. Based on this, a discontinuous control algorithm was presented in [1]. Furthermore, that control law offered some advantages: it is an output feedback algorithm, easy to implement and cheap in terms of computational time. The designed controller yields a closed loop dynamics that leaves invariant a subset of a cylinder on which there are two locally asymptotically stable equilibrium points. However, the full dynamics is complex and this complexity increases when some constrains of the actual WRSG are considered.
The paper is organized as follows: next Section summarizes the system description and the control design procedure obtained in [1]. Local stability is proved and the basin of attraction is determined. A more real scenario, considering bounds in the value of the voltages applied to the WRSG is analyzed, and experimental results are presented. Finally, the conclusions are drawn.

System description and control design

The dynamics of a sliding mode controlled WRSG is outlined here. For further details about the model and the control design, the reader is referred to [1].
Stand-alone wound rotor synchronous machine can be modeled by the linear system

$$L\frac{\mathrm{d}x}{\mathrm{d}t} = Ax + Bv_F, \tag{1}$$

where,

$$L = \begin{pmatrix} L_s & 0 & L_m \\ 0 & L_s & 0 \\ L_m & 0 & L_F \end{pmatrix},$$

$$A = \begin{pmatrix} -(R_s+R_L) & \omega L_s & 0 \\ -\omega L_s & -(R_s+R_L) & -\omega L_m \\ 0 & 0 & -R_F \end{pmatrix},$$

and

$$B = \begin{pmatrix} 0 \\ 0 \\ 1 \end{pmatrix}.$$

State components, $x^T = (i_d, i_q, i_F) \in \mathbb{R}^3$ are the dq-stator and field currents respectively, L is the inductance matrix and A collects the dissipation and the interconnection matrices. Finally, v_F is the field voltage that will be used as a control input. Although the system is linear, the desired output, which corresponds to the stator voltage amplitude

$$V_s = \sqrt{v_d^2 + v_q^2} = R_L\sqrt{i_d^2 + i_q^2}. \tag{2}$$

is highly non-linear. System (1) has a straight line of equilibrium points, l_{eq}, parametrized by v_F, defined as,

$$l_{eq}^{*T}(v_F) = \left(-\frac{\omega^2 L_s L_m}{R_F|Z_s|^2}, -\frac{\omega L_m(R_s+R_L)}{R_F|Z_s|^2}, \frac{1}{R_F}\right) v_F \tag{3}$$

where $|Z_s|^2 = \omega^2 L_s^2 + (R_s + R_L)^2$.
According to the desired output (2) the following switching function was proposed:

$$s(x) = V_s^2 - V_{ref}^2 = R_L^2(i_d^2 + i_q^2) - V_{ref}^2. \tag{4}$$

$s(x) = 0$, results in a cylinder centered at the origin, with base radius $\frac{V_{ref}}{R_L}$. The desired equilibria lie in the intersection of the straight line,l_{eq}, with the cylinder $s(x) = 0$, Fig. 1.

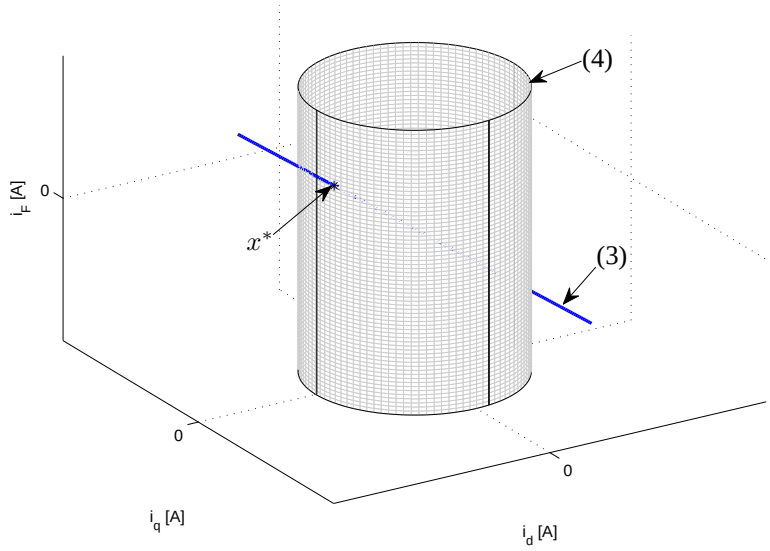

Figure 1: Intersection of the control goals and the equilibrium points distribution of the system.

As usual in SMC, in order to have sliding modes on $s(x) = 0$ we define a discontinuous control action v_F so that $s \cdot \frac{ds}{dt} < 0$. Standard computations to design the control action involve the equivalent control[1] [3] and take benefit of the sign of some expressions. It results a bang-bang control voltage defined by

$$v_F = \begin{cases} -V_{DC} & \text{if } s\, i_d < 0 \\ V_{DC} & \text{if } s\, i_d > 0 \end{cases} \tag{5}$$

which is independent of the plant parameters and of the load value. The closed loop dynamics possess sliding modes on the sliding domain (the subset of $s = 0$ defined by $-V_{DC} < u_{eq} < V_{DC}$). Note that the higher the voltage V_{DC}, the wider the sliding domain on the cylinder.

Analysis of the ideal sliding dynamics

This section deals with the ideal sliding dynamics (ISD), *i.e.* the dynamics on the cylinder presumed that there are sliding modes on it and there are no constrains on the control action v_F so that trajectories achieve the cylinder in finite time. The ISD is analyzed in polar coordinates and local stability of the equilibrium points is proved thanks to the Poincaré-Bendixon and Bendixon theorems. As an additional consequence of the proof, the basin of attraction is obtained. Requiring sliding modes on the cylinder is equivalent to it is flow invariant by the, ideally at infinite frequency, discontinuous dynamics. This condition is satisfied in the cylinder subspace defined by $i_d \neq 0$. Taking cylindrical coordinates in $\mathbb{R}^3$, (I, δ, i_F) where $i_d = I\cos\delta$, $i_q = I\sin\delta$, and replacing v_F by the equivalent control in (1), the invariant dynamics on $s = 0$ results in

$$\cos\delta \frac{\mathrm{d}\delta}{\mathrm{d}t} = -a i_F - b\sin\delta - \omega\cos\delta \tag{6}$$

$$\cos\delta \frac{\mathrm{d}i_F}{\mathrm{d}t} = -\omega i_F \sin\delta - c. \tag{7}$$

where $a = \frac{\omega L_m R_L}{V_{ref} L_s}$, $b = \frac{R_s + R_L}{L_s}$ and $c = \frac{R_s + R_L}{L_m R_L} V_{ref}$.

[1] The equivalent control u_{eq} is computed through $\frac{\mathrm{d}s}{\mathrm{d}t} = 0$.

Remarks

- The equilibrium points (δ^*, i_F^*) are the points where the cylinder $s = 0$ and the straight line of equilibrium points cross. These points are also the equilibria of the ISD (6)-(7). Solving (7) for i_F, replacing the solution in (6) and using some algebra yields

$$b\cos\delta^* - \omega\sin\delta^* = 0.$$

  Thus,

$$\delta^* = \arctan\left(\frac{b}{\omega}\right) = \arctan\left(\frac{R_s + R_L}{\omega L_s}\right) \tag{8}$$

  which has a unique solution δ^* in $(-\frac{\pi}{2}, \frac{\pi}{2})$. Then, the field current equilibrium values are

$$i_F^* = -\frac{V_{ref}}{\omega L_m R_L}(\omega L_s \cos\delta^* + (R_s + R_L)\sin\delta^*), \tag{9}$$

  and the control value, obtained from (1) yields

$$v_F^* = -\frac{R_F}{\omega L_m R_L} V_{ref}(\omega L_s \cos\delta^* + (R_s + R_L)\sin\delta^*).$$

  Note that $v_F^* = u_{eq}(i_d^*, i_q^*, i_F^*)$. The eigenvalues of the Jacobian of the Ideal Sliding Dynamics are in the left-half plane. Hence the equilibrium points are locally asymptotically stable.

- The dynamics is not defined in $\delta = \pm\frac{\pi}{2}$ (which corresponds to $i_d = 0$).

- There is a symmetry in the system. The sliding domain, *i.e.* the complementary of the planes $i_d = \pm\frac{\pi}{2}$ in the cylinder, has two connected components. The diffeomorphism $\phi(\delta, i_F) = (\delta + \pi, -i_F)$ transforms the dynamics on the subset of the cylinder defined by $\delta \in (-\frac{\pi}{2}, \frac{\pi}{2})$ into the dynamics on the subset of the cylinder defined by $\delta \in (\frac{\pi}{2}, \frac{3\pi}{2})$.

- The phase-portrait of the ISD on the cylinder is shown in Figure 2(a). The normalized vector field, two trajectories and the basin of attraction of the dynamical system defined by (8) and (9) are depicted. The cylinder is obtained by identifying the straight lines of the border of the strip $-\frac{\pi}{2} < \delta < \frac{3\pi}{4}$. The sliding domain has two connected components, namely $-\frac{\pi}{2} < \delta < \frac{\pi}{2}$ and $\frac{\pi}{2} < \delta < \frac{3\pi}{4}$. Note the symmetry already reported. Figure 2(a) also shows two subsets of the sliding domain where trajectories do not converge to the equilibria (these two areas are delimited by gray lines).

- The gray curve in Figure 2(a) trough points p, $\bar{p}$ and p is a limit cycle of the ISD.

- Thanks to the Poincaré-Bendixon and Bendixon theorems we can state that the ISD basin of attraction of each of the equilibrium points is the bounded domain of the cylinder limited by the limit cycle.

- In a real application, the V_{DC} values are restricted by the voltage source, or the nominal values of the power converter. The main consequence of saturated V_{DC} values is that the sliding condition fulfills in a strict subset of the switching surface $s(x) = 0$ defined by

$$\left|\frac{\mu}{2L_m R_L^2}\frac{1}{i_d}\left(\frac{\partial s}{\partial x}L^{-1}Ax\right)\right| < V_{DC}, \tag{10}$$

  actually a very small subset. Sliding domains in the (δ, i_F) of the cylinder for a WRSG and two different values of V_{DC} are depicted in Figure 2(b) . Note that the higher the V_{DC} value, the wider the sliding domain.

Experimental results

A scheme of the experimental test bench is shown in Figure 3. A DC motor drags the WRSG which rotor position and stator voltages are measured. These measurements are acquired by a Digital Signal Processor (DSP), which is programmed from a personal computer. By using a rectifier and a capacitor, the grid voltage is rectified from AC to DC and a DC/DC power converter is used to apply the control defined by the DSP card to the WRSG. The DC motor is a 3kW machine and is used to fix the WRSM mechanical speed at 1500rpm (which corresponds to 50Hz stator frequency) with the 4Q2 Control Techniques Drives Ltd commercial speed controller. The power converter is a full bridge DC/DC converter which can provide $\pm V_{DC}$ voltages. The bus voltage is set to $V_{DC} = 137.5$V for the experimental tests. The resistive load is a bank, with full load value (equivalent to $R_L = 64\Omega$ for the nominal voltage).
The WRSG is a 2.4kVA, 4 pole three-phase machine. Nominal characteristics and parameters obtained using IEEE Std. 115-1995 are in Table 1[2].

[2]The apostrophe indicates that the parameters are referred from the rotor to the stator and that n is the transformation relationship

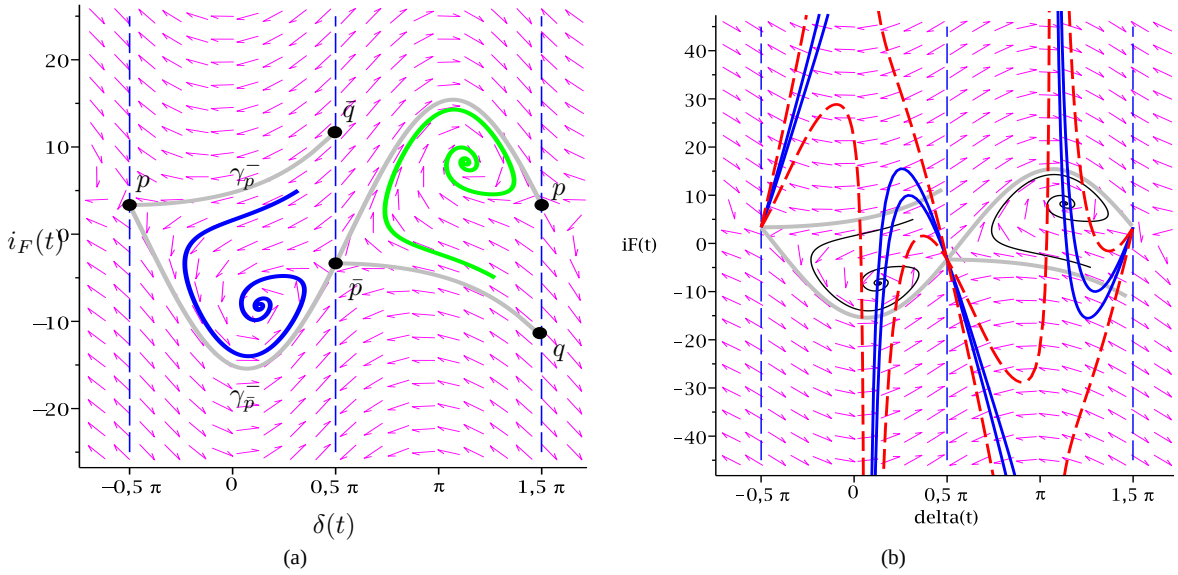

Figure 2: a) State space: vector field and two trajectories for different initial conditions. b) Sliding zones for limited V_{DC} value.

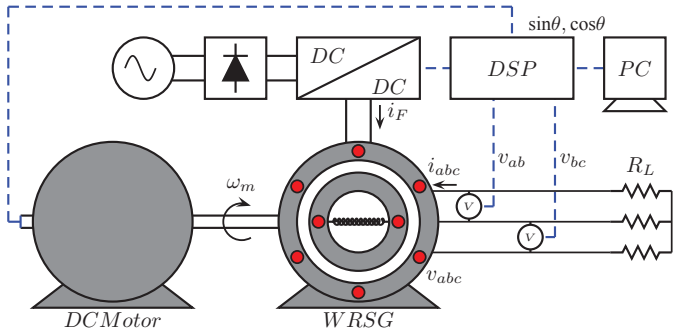

Figure 3: Scheme of the experimental test bench.

The experimental test consist of changing the reference value of the stator voltage amplitude, V_{ref}. The v_d, v_q, i_F signals are acquired and displayed. Also, the dq-voltages and the field current signals are plotted in a 3D figure, similarly to the fixed point study, Fig. 1. Notice that the signals contain some noise measurements which implies that equilibria are converted to a bounded region (specially when the 3D plot is obtained).

Several test were performed changing the initial and the final voltage references, and different transient behavior were obtained. In the paper, two illustrative cases are presented.

The first test corresponds to a change of the reference from $V_{ref} = 250$V to $V_{ref} = 380$V, Fig. 4(a) and 4(b). The experimental results show that the stator voltage amplitude is regulated with a small time response. The switching function jumps out the sliding surface after the reference change, but it slides again after less than one cycle. The 3D plot shows the state evolution in terms of v_d, v_q and i_F. The two cylinders corresponding to the sliding surfaces for each reference value are also plotted. In this case, the system moves from the inner cylinder to the external one following the shortest path.

In the second experiment the stator voltage amplitude reference changes from $V_{ref} = 370$V to $V_{ref} = 270$V, Fig. 5(a) and 5(b). In this case the obtained behavior is quite different to the previous test. Notice that the stator voltage amplitude is reached after some attempts. The fact here is that the system cannot keep on the sliding surface due to the limits found in (8). Once the sliding condition is lost, the system goes to equilibria of (1) for a constant value of v_F ($+V_{DC}$ or $-V_{DC}$) which is located in the opposite side of the cylinder. This behavior can occur several times. Figure 5(a) shows how the system switches three times of the final equilibria. Also, the 3D plot, in Fig. 5(b), points out that the system trajectory is

$f = 50$Hz	$n = 1500$rpm	$P = 2.4$kVA
3ph	Δ/Y	$V_F = 100$V
$I_F = 2.4$A	$V_s = 220/380$V	$I_s = 6.3/3.65$A
$R_s = 3.06\Omega$	$L_s = 0.48$H	$R_F = 39.65\Omega$
$L_m = 0.31$H	$L_F = 3.87$H	$n = 4$
$R'_F = 2.48\Omega$	$L'_F = 0.24$H	

Table 1: WRSG data characteristics and parameters.

a straight line between the two equilibria.

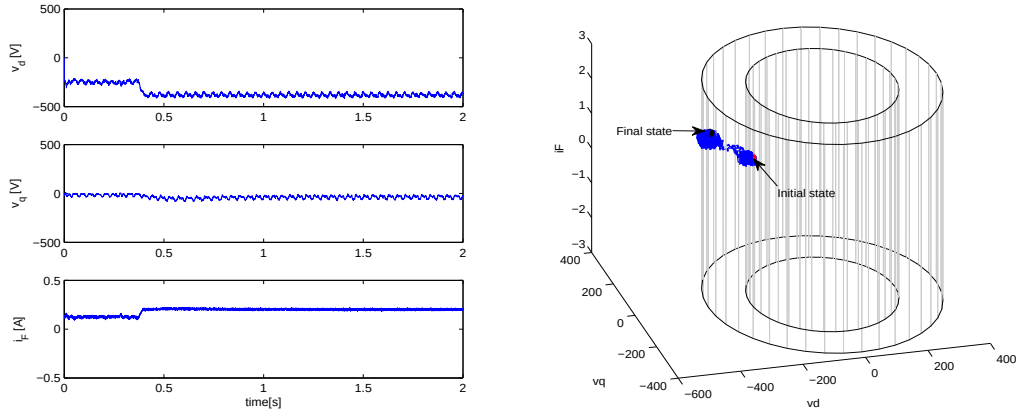

(a) (b)

Figure 4: Experimental results: a) States and b) trajectory behavior for a reference change from $V_{ref1} = 250V$ to $V_{ref2} = 380V$.

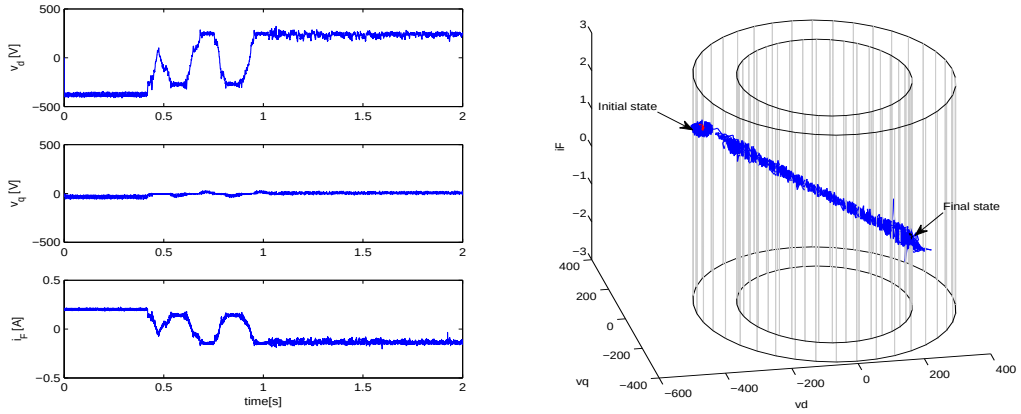

(a) (b)

Figure 5: Experimental results: a) States and b) trajectory behavior for a reference change from $V_{ref1} = 370V$ to $V_{ref2} = 270V$.

Acknowledgments

R. S. Muñoz-Aguilar and A. Dòria-Cerezo were partially supported by the Spanish government research projects ENE2008-06841-C02-01/ALT and DPI2010-15110, respectively, while E. Fossas was also partially supported by the Spanish government research projects DPI2010-15110 and DPI2008-01408.

Conclusions

The closed loop dynamics of a sliding mode controlled WRSG is reported here. Assuming higher enough DC-voltages V_{DC} there are sliding modes on the system. Poincaré-Bendixon and Bendixon theorems allow us to prove that the ideal sliding dynamics on the cylinder consists in two locally asymptotically stable equilibrium points and the whole dynamics presents limit cycles. The case of saturated values of V_{DC} is also studied. This realistic case reveals that the sliding condition holds in some narrow strips only. However, these strips are wide enough to guarantee local stability of the equilibrium points. Experimental tests show a very rich transient behavior which contain two sliding regions where the trajectories can jump from one to other before to reach the sliding surface and the final equilibrium point defined on it.

References

[1] R.S. Muñoz-Aguilar, A. Dòria-Cerezo, E. Fossas, and R. Cardoner. Sliding mode control of a stand-alone wound rotor synchronous generator. *IEEE Trans. on Industrial Electronics, DOI: 10.1109/TIE.2011.2116754*, 2011.

[2] V. Utkin, J. Guldner, and J. Shi. *Sliding Mode Control in Electromechanical Systems*. Taylor and Francis, 1999.

[3] V.I. Utkin. *Sliding Modes and their Applications in Variable Structure Systems*. Mir. Moscow, 1978.